A Thyristor-Based Reliable Bidirectional SSCB With Fast-Reclosing Protection Function

Kejun Qin, *Student Member, IEEE*, Shunliang Wang, *Member, IEEE*, Junpeng Ma, *Member, IEEE*, Ji Shu, Rui Zhang, *Student Member, IEEE*, and Tianqi Liu, *Senior Member, IEEE*

***Abstract*—Due to numerous advantages of thyristors, such as low conduction loss and low cost, using thyristors to design solid-state circuit breakers (SSCBs) to protect dc microgrids has become increasingly popular. However, the majority of existing bidirectional thyristor-based SSCBs (TCBs) have one or more following drawbacks: high conduction loss, lack of operating current interrupting ability, low current breaking reliability, unsuitable for fast-reclosing protection, and the need to use ample thyristors. To address these problems, a new bidirectional TCB is proposed in this article. First, the proposed method could break both bidirectional operating and fault currents reliably by actively turning ON its auxiliary thyristors. Second, the conduction loss of the proposed TCB is extremely low. Third, the proposed TCB can realize fast-reclosing protection function by masterly using an *LC* resonant circuit, which would ensure a safe restart of dc microgrids after a fault. Finally, the proposed TCB is very economical since only one additional set of auxiliary parallel thyristors is needed. Thus, all the above merits are making the proposed TCB a promising candidate for protecting dc microgrids. The parameter design guidelines, scaled-down experimental results, and comparative studies of the proposed TCB are also presented.**

***Index Terms*—DC microgrid, dc system, short-circuit protection, solid-state dc circuit breaker (SSSCB), thyristor.**

I. Introduction

IT HAS been increasingly demonstrated that dc microgrids are superior to ac systems in a lot of aspects, such as having a higher efficiency, simpler control, lower cost, and higher reliability [1]. Besides, with the development of many modern applications (e.g., solar photovoltaic, wind power generation technology, and electric vehicle charge stations), the dc microgrids are further promoted and reinforced [2], [3], [4], [5]. However, unlike the fault current in ac systems after a fault, the dc fault current in dc microgrids rises rapidly, and there is no natural current zero-crossing point [6].

Because of fast reaction speed, easy intelligent control, and arc-free operation process, adopting solid-state circuit breakers (SSCBs) has been widely recognized as one suitable method to protect dc microgrids by quickly and selectively isolating a faulty part from healthy areas [7], [8]. From the point of view of practicality, there are three basic functions that SSCB should possess [2], [3] are as follows:

1) it could interrupt the operating current in normal condition during microgrid maintenance;
2) it should reliably interrupt the bidirectional fault current due to the diversity of power flow;
3) fast-reclosing operations are often adopted to reduce the damage caused by a temporary fault. Thus, SSCBs should break the fault current reliably again after reclosing, which could provide a safe restart for dc microgrids.

SSCBs based on full-controllable devices, such as Si IGBTs and SiC MOSFETs, have been widely researched for their simple structures and high current breaking reliability [9], [10]. Although SSCBs based on full-controllable devices can easily satisfy the three basic functions, they sacrifice conduction loss and construction cost. The semicontrollable device thyristor and thyristor-derived devices are also suitable devices for designing SSCBs due to their advantages, such as high surge current carrying capacity and low ON-state resistance [11]. Yet the cost of thyristor-derived devices is generally higher than that of thyristors due to additional special circuit designs. Finally, thyristors are more suitable for designing SSCBs in the aspects of cost and loss. Since thyristor is semicontrollable, the key issue that thyristor-based SSCBs (TCBs) need to solve is the turning OFF of the thyristors. Based on whether TCBs can actively send current breaking signals, existing TCBs could be broadly divided into two types: passive TCBs and active ones.

So far, numerous passive TCBs, represented by Z source circuit breakers, have been widely researched [12], [13], [14]. These passive TCBs without current sensing procedures are all triggered after fault. By arranging the Z-source structure or coupled inductors reasonably, a reverse voltage or current could be automatically generated across the thyristor after a fault, and then, the thyristor will be turned OFF automatically. The topologies in [12], [13], and [14] are all unidirectional, which limits

Manuscript received 1 November 2022; revised 10 March 2023 and 20 July 2023; accepted 30 August 2023. This work was supported by the Natural Science Foundation of Sichuan Province under Grant 2023NSFSC0301 and in part by the Natural Science Foundation of Sichuan Province under Grant 2022NSFSC1904. *(Corresponding author: Shunliang Wang.)*

Kejun Qin, Shunliang Wang, Junpeng Ma, Rui Zhang, and Tianqi Liu are with the College of Electrical Engineering, Sichuan University, Chengdu 610065, China (e-mail: qkj1997@stu.scu.edu.cn; slwang@scu.edu.cn; jma@scu.edu.cn; rui_zhang@stu.scu.edu.cn; tqliu@scu.edu.cn).

Ji Shu is with the Department of Electronic and Computer Engineering, The Hong Kong University of Science and Technology, Hong Kong (e-mail: jay.shu@connect.ust.hk).

Color versions of one or more figures in this article are available at https://doi.org/10.1109/TIE.2023.3319725.

Digital Object Identifier 10.1109/TIE.2023.3319725

their application in dc microgrids, where bidirectional power flow is often required. As a result, these topologies do not achieve the second function, i.e., they could not break the bidirectional fault current. To solve this problem, some improved bidirectional passive TCBs are proposed by rational configuration [15], [16], [17], [18]. Yet these bidirectional passive TCBs generally have following four common issues.

1) *High Conduction Loss:* Since TCB is a kind of long-term conducting equipment, conduction loss is one key property. As illustrated in [11], from the perspective of reducing conduction loss, the most ideal connection method is to place only one set of parallel thyristors in the conducting branch. Thus, these bidirectional passive TCBs, except the one in [18], all sacrifice conduction loss for bidirectional breaking ability.
2) *Low Controllability (corresponding to the first function of SSCB):* The low controllability, here, means that these passive TCBs could not actively send signals that break the current since they only work after a fault occurs. Thus, they cannot interrupt the normal operating current. One simple and direct solution is adding active severe artificial faults to simulate natural faults to trigger these TCBs. Yet the negative damage caused by manual faults to the grids can also occur as natural one does. In addition, if manual faults triggering method is used, the operation procedures in normal and fault current breaking processes are plainly different, which will make the whole control system more complex.
3) *Low Reliability (corresponding to the second function of SSCB):* Since all these passive TCBs are generally designed under ideal situations, i.e., without considering the changeable and inaccessible parasitic parameters of an outer circuit, the reliability of their fault current breaking processes could not be ensured when used in real conditions. Furthermore, the current breaking reliability is one important feature that SSCBs should possess because if breakers are unreliable, breakers could not accomplish its role (i.e., interrupting the fault) competently. In addition, since the operating current may change significantly when the power flow of a grid fluctuates, passive TCBs may be triggered by mistakes, which is also a type of low reliability.
4) *Unsuitable for Fast Reclosing (corresponding to the third function of SSCB):* Capacitors are often needed in TCBs to help turning OFF thyristors. For turning OFF thyristors successfully after reclosing, the states of capacitors in a reclosing protection process should be the same as those in the initial one. Unfortunately, the capacitors in [15], [16], and [18] could only be charged after reclosing process starts. Thus, these passive TCBs are unable to guarantee fast-reclosing protection function. For the topology in [17], the capacitor energy will decrease after the first current breaking process, which may weaken the reclosing protection reliability.

In addition to these passive TCBs, some active TCBs are also proposed. Since they could actively send triggering signals to auxiliary switches, the low controllability problem can be solved. Two active TCBs are proposed in [19] and [20], which do not have the ideal lowest conduction loss. In addition, their current breaking reliability could not be ensured because the loops for turning OFF their thyristors include the outer line circuit. Based on the operational principles illustrated in [21], one capacitor in the TCB in [21] should be zero voltage and the other fully charged. However, such an asymmetrical circuit arrangement may threaten bidirectional current breaking reliability since capacitors need time to charge or discharge. In addition, since capacitors need to discharge energy through their paralleled huge resistors after the first current breaking process, the time requirement for fast reclosing may not be satisfied due to the large *RC* time constant. To solve the current breaking reliability issue, five active and bidirectional TCBs are proposed in [22], [23], [24], [25], and [26]. Two smart TCBs for decreasing the surge current to both the source and load sides are proposed in [22] and [23]. Yet they still carry high conduction loss as does the topology in [24]. In addition, the turn-OFF process of the auxiliary thyristors in the TCB in [22] and [23] are not considered in detail, and failure of turning OFF the auxiliary thyristor will lead to a failure of reclosing protection. Two reliable TCBs with the ideal lowest conduction loss are proposed in [25] and [26]. The TCB in [25] only considers the first current breaking process. Moreover, the capacitors of the TCB in [25] will be charged slowly after reclosing because of its enormous charging resistor, which makes this TCB not suitable for a fast-reclosing protection. The auxiliary thyristors in the TCB in [26] have the possibility to be turned OFF unsuccessfully if the charging resistors in [26] are small. If so, a fast-reclosing protection will not be guaranteed. In addition, ample thyristors are needed in the topologies in [24] and [26], which makes the TCBs expensive.

For solving the issues appeared in the above TCBs, a new bidirectional TCB used for dc microgrids is introduced in this article, which can simultaneously satisfy the three basic functions that a SSCB should possess. Full controllability and high current breaking reliability are ensured through intelligent control, which indicates that it can break both bidirectional operating and fault current actively and reliably. The proposed TCB could also realize fast-reclosing protection function by masterly using an *LC* resonant circuit. In addition, there are only two sets of parallel thyristors in the breaker. One is placed in the main branch and the other auxiliary branch. As a result, both conduction loss and construction cost are remarkably low. Ultimately, the key contribution of this topology is showing the novel aspect of how to use an *LC* resonant circuit to realize a reliable fast-reclosing protection, which has not been considered in former works about TCBs.

II. Proposed Topology

A. Topology Introduction

The proposed topology is presented in Fig. 1. RCB_m is a residual current breaker (RCB), which could isolate the fault physically after the current breaking process. Moreover, limiting reactor L_m could limit the current rising rate after fault according to the system protection requirements.

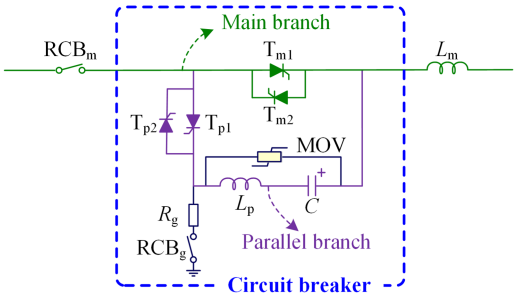

Fig. 1. Proposed TCB.

There are two branches in the proposed TCB, which are the main branch and the parallel branch, respectively. There is only one set of parallel thyristors, including T_{m1} and T_{m2}, in the main branch. Thus, the bidirectional conducting capability is ensured, and the conduction loss is low. As a result, system efficiency is high. The parallel branch consists of inductor L_p, capacitor C, and two parallel thyristors including T_{p1} and T_{p2}. The capacitor C could be fully charged through the big grounded resistor R_g from the dc source. Furthermore, RCB_g keeps on in normal condition to provide the charging path for capacitor C. It should be noted that the RCB_g has the same specifications as RCB and keeps low costs. Finally, the metal oxide varistor (MOV) could dissipate the system energy and protect thyristors in the proposed TCB.

Since the proposed TCB is an asymmetrical structure, the forward and backward current breaking principles are different. The two principles are elaborated in parts B and C of Section II.

B. Forward Current Breaking Principles

The detailed forward current breaking principles of the proposed TCB are shown in Fig. 2, where R_l is the dc load.

1) *Mode I_f—Normal Operating Condition:* The thyristor T_{m1} is in a conduction state and conducts operating current I_{m_f}. Meanwhile, the capacitor C is charged to dc source voltage V_s.
2) *Mode II_f—Fault Occurs:* After fault occurs, the fault current I_{m_f} rises. Since the duration of this mode is short and the resistor R_g is rather large, the voltage drop of capacitor C in this mode is negligible.
3) *Mode III_f—Thyristor T_{p1} turns ON, and RCB_g switches OFF:* After the current I_{m_f} reaches the preset operation value I_{f0}, the proposed TCB proceeds (i.e., simultaneously turning ON the thyristor T_{p1} and switching OFF the RCB_g). When the thyristor T_{p1} is turned ON, one counter current I_{PB_f} and one leakage current I_{g_f} caused by R_g will be generated. Then, the RCB_g switches OFF to interrupt this leakage current I_{g_f}.
4) *Mode IV_f—Thyristor T_{m1} undergoes a reverse recovery process:* After the current I_{PB_f} increases to be equal to current I_{m_f}, the thyristor T_{m1} will undergo a reverse recovery process.
5) *Mode V_f—Capacitor Charges and MOV is Triggered to Dissipate System Energy:* After mode IV_f, the thyristor T_{m1} has been turned OFF successfully. Then, the capacitor C will be charged reversely by fault current I_{m_f}. In addition, the MOV will be triggered to dissipate system energy when its threshold voltage is reached.
6) *Mode VI_f—Steady State before Reclosing:* After the main branch current I_{m_f} reaches zero, the thyristor T_{p1} will be turned OFF automatically. Ultimately, the polarity of capacitor C has flipped, and the absolute value of capacitor voltage has been equal to or higher than the source voltage V_s. Since the RCB_g has been OFF, capacitor C has no discharging path, and the capacitor voltage keeps stable.
7) *Mode VII_f—Reclosing Process Begins, and Thyristors T_{m1} and T_{p2} turn ON Simultaneously:* When the reclosing process begins, turn-ON signals are sent to thyristors T_{m1} and T_{p2} simultaneously. Then, a round of LC resonance begins.
8) *Mode $VIII_f$—Polarity of C flips and Capacitor C Returns to the Initial State:* After half an LC resonance period, the polarity of capacitor C is flipped again to the initial state. It should be noted that the reverse recovery duration of the thyristor T_{p2} is also necessary before the proposed TCB reacts. Since only half of an LC resonance period is needed, and the internal circuit impendence is small, the capacitor voltage drop in the flipping duration is miniscule that it could be neglected.

The highlight of the forward current breaking principle is how the fast-reclosing protection function is implemented. The capacitor polarity restores to the initial state through LC resonant circuit by utilizing the moment when reclosing starts, that is, when thyristor T_{m1} is turned ON. Then, the proposed TCB could break the fault current again after reclosing if permanent fault exists.

C. Backward Current Breaking Principles

The detailed backward current breaking principles of the proposed TCB are shown in Fig. 3.

1) *Mode I_b—Normal Operating Condition:* The thyristor T_{m2} is in a conduction state and conducts operating current I_{m_b}. Meanwhile, the capacitor C is charged to dc source voltage V_s.
2) *Mode II_b—Fault Occurs:* After fault occurs, fault current I_{m_b} rises. Since the duration of this mode lasts only momentarily, and the resistor R_g is rather large, the voltage drop of capacitor C in this mode is negligible too.
3) *Mode III_b—Thyristor T_{p1} turns ON, and RCB_g switches OFF:* After the current I_{m_b} reaches the preset operation value I_{f0}, the proposed TCB proceeds (i.e., simultaneously turning ON the thyristor T_{p1} and switching OFF the RCB_g). However, different from the function of mode III_f, this mode aims to flip the capacitor polarity in advance.
4) *Mode IV_b—Polarity of C Flips, and the Thyristor T_{p1} is Turned OFF Automatically:* After half of an LC resonance period, the polarity of the capacitor is flipped. Then, a

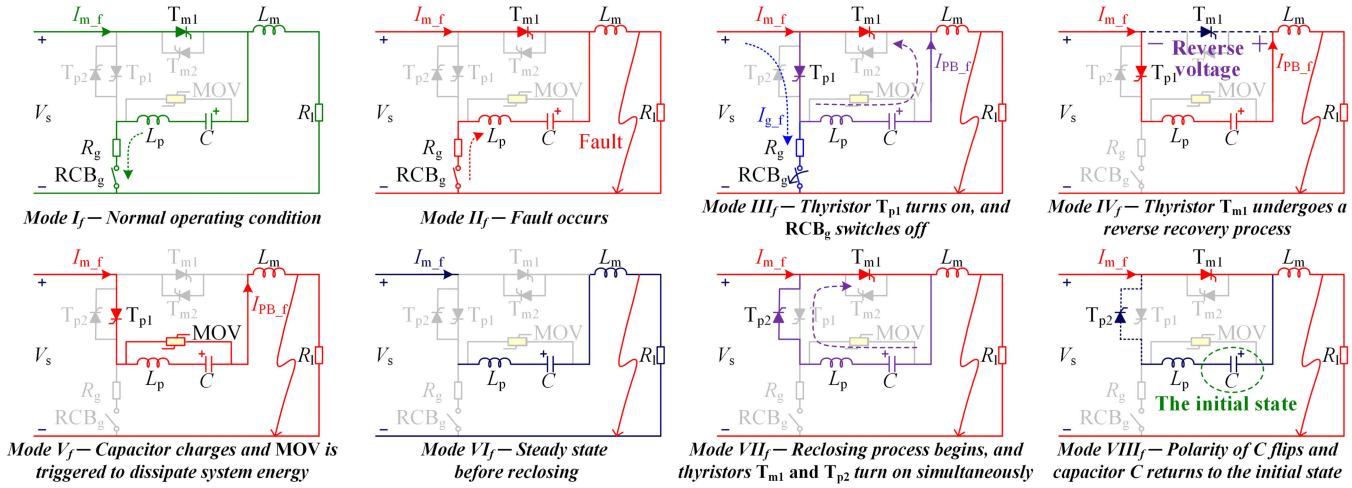

Fig. 2. Forward current breaking principles of the proposed TCB.

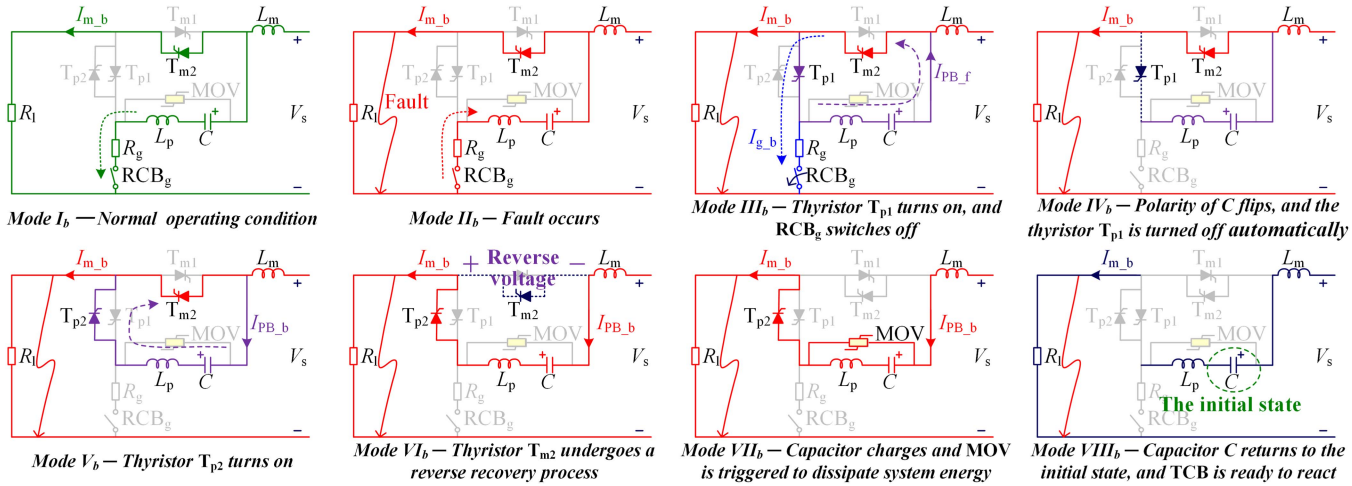

Fig. 3. Backward current breaking principles of the proposed TCB.

short duration is needed for the thyristor T_{p1} to recover reversely. Since the *LC* resonance frequency could be chosen to be several kilohertz or even tens of kilohertz, the additional half an *LC* resonance period is transient. In addition, a thyristor with a short reverse recovery duration (several tens of μs) could be selected. Therefore, for flipping the capacitor polarity, the extended duration caused by modes III_b and IV_b is necessary and acceptable.

5) *Mode V_b—Thyristor T_{p2} Turns ON:* After mode IV_b, the thyristor T_{p1} has been turned OFF. The turn-ON signal is then sent to the thyristor T_{p2}. Similar to mode III_f, a counter current I_{PB_b} is generated.
6) *Mode VI_b—Thyristor T_{m2} Undergoes a Reverse Recovery Process:* After the current I_{PB_b} increases to become equal to the current I_{m_b}, the thyristor T_{m2} will undergo a reverse recovery process.
7) *Mode VII_b—Capacitor Charges and MOV is Triggered Todissipate System Energy:* After mode VI_b, the thyristor T_{m2} has been turned OFF successfully. Then, the capacitor *C* will be charged reversely by the fault current I_{m_b}. Besides, the MOV will be triggered to dissipate system energy when reaching its threshold voltage.
8) *Mode $VIII_b$—Capacitor C Returns to the Initial State, and TCB is Ready to React:* After the main branch current I_{m_b} reaches zero, the thyristor T_{p2} will be turned OFF automatically. Ultimately, the polarity of capacitor *C* has returned to the initial state, and the absolute value of capacitor voltage has been equal to or higher than the source voltage V_s. Since the RCB$_g$ has been OFF, capacitor *C* has no discharging path, and the capacitor voltage keeps stable.

D. Operation Sequences

According to the aforementioned principles, the flowchart of the protection sequences is illustrated in Fig. 4, where two sensing and current breaking processes are considered. As illustrated in Sections II-B and II-C, both the currents I_{m_f} and I_{m_b} are

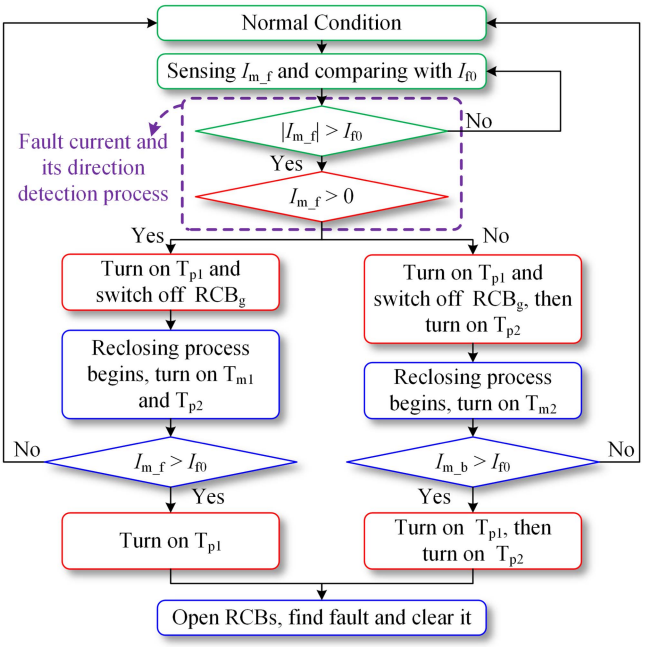

Fig. 4. Flowchart of the operation sequences.

the main branch current, but their directions are the opposite. Since the operation principles of bidirectional current breaking processes are totally different, the fault current and its direction detection process, as marked in Fig. 4, are added.

III. Parameters Designing Guidelines

The most important issue when designing parameters for the proposed TCB is to ensure that the thyristors in the main branch can be turned OFF reliably. The duration when the thyristors undergo reverse voltage (Δt) should be longer than the recovery time of thyristor (t_r), even in the most severe condition. To guarantee a reliable breaking ability, there are two situations needed to be considered. They are the first current breaking process and the breaking process after reclosing, respectively.

A. Requirements for the First Current Breaking Process

Compared with the forward current breaking process, both an additional half an *LC* resonance period and the reverse recovery process for thyristor T_{p1} are necessary before turning OFF the thyristor T_{m2} in the backward current breaking process, as shown in modes III_b and IV_b of Fig. 3. The sum of them is t_{add}, as shown in (1). Hence, when the turn-ON signal is sent to thyristor T_{p2} in the mode V_b, the fault current I_{m_b} becomes bigger than preset value I_{f0}. Therefore, the reliability of this situation is lower and needs to be considered. Two modes including mode V_b and mode VI_b are analyzed here to study the requirements for the reliable first current breaking process. In addition, the effect of the outer circuit parameter is also considered. A simplified parameter L_{out} is added in Fig. 5, which equals to zero when a fault occurs at the output of the proposed TCB. As fault distance

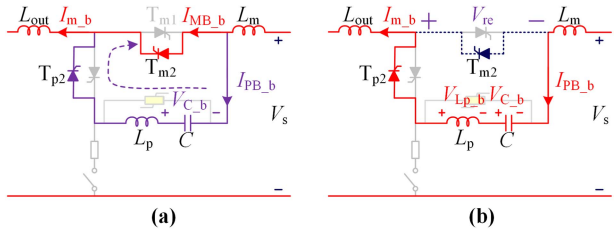

Fig. 5. Circuit analysis of the modes V_b and VI_b after thyristor T_{p2} is turned ON in the backward current breaking process. (a) Mode V_b (t_1–t_2). (b) Mode VI_b (t_2–t_3).

increases, L_{out} increases.

$$t_{add} = t_r + \pi\sqrt{L_p C}. \tag{1}$$

1) Mode V_b (t_1–t_2): The mode V_b shown in Fig. 5(a) is analyzed first. Assuming the timepoint when the turn-ON signal is sent to the thyristor T_{p2} in the mode V_b is t_1, the current I_{m_b} could be calculated as

$$I_{m\_b} = I_{f0} + \frac{V_s}{L_{out} + L_m}(t_{add} + t - t_1). \tag{2}$$

After thyristor T_{p2} is turned ON, the current I_{PB_b} is

$$I_{PB\_b} = \sqrt{\frac{C}{L_p}} V_s \sin\frac{t - t_1}{\sqrt{L_p C}}. \tag{3}$$

Then, the current I_{MB_b} flowing through thyristor T_{m2} could be expressed as follows:

$$I_{MB\_b} = I_{m\_b} - I_{PB\_b}. \tag{4}$$

Hence, the timepoint t_2 could be calculated by

$$t_2 = t|_{I_{MB\_b}=0}. \tag{5}$$

Then, current I_{m_b} and voltage V_{C_b} can be obtained as

$$I_{m\_b}(t_2) = I_{m\_b}|_{t=t_2} = A \tag{6}$$

$$V_{C\_b}(t_2) = V_s \cos\frac{t - t_1}{\sqrt{L_p C}}\bigg|_{t=t_2} = B. \tag{7}$$

Since the duration (t_2–t_1) is short, (4) could be simplified by Taylor expansion

$$I_{MB\_b} = I_{f0} + \frac{V_s t_{add}}{L_{out} + L_m} + \left(\frac{V_s}{L_{out} + L_m} - \frac{V_s}{L_p}\right)(t - t_1). \tag{8}$$

For ensuring reliable current commutation from the main branch to the parallel branch, current I_{MB_b} needs at least one zero current crossing point. The corresponding function image of (8) is a direct line, and the function value at time t_1 is positive. Thus, the slope needs to be negative. Then, the following can be obtained:

$$L_p < (L_{out} + L_m). \tag{9}$$

2) Mode VI_b (t_2–t_3): The mode VI_b shown in Fig. 5(b) is analyzed here. After the mode V_b, the current I_{MB_b} flowing through the thyristor T_{m2} is zero. Then, as shown in Fig. 5(b),

the thyristor T_{m2} undergoes the reverse voltage V_{re} in the mode VI_b. V_{Lp_b} is the voltage across the inductor L_p, and V_{C_b} is the residual voltage of capacitor C. The sum of V_{Lp_b} and V_{C_b} is the reverse voltage V_{re} undertook by the thyristor T_{m2}.

The voltage V_{Lp_b} at timepoint t_2 could be calculated by

$$V_{Lp\_b} = \frac{-L_p}{L_p + L_m + L_{out}} (V_s + B). \tag{10}$$

The function of inductor L_p is to generate one massive current, and that of inductor L_m is to limit the fault current rising rate. Generally, L_p is in the order of μH, and L_m is in the order of mH. Hence, (9) and (11) are always satisfied, and the V_{Lp_b} shown in (10) is always miniscule, which can be neglected. Consequently, the reverse voltage V_{re} undertook by the thyristor T_{m2} is mainly generated by the residual energy of capacitor C.

$$L_m \gg L_p. \tag{11}$$

Since the reverse recovery process of thyristor T_{m2} is momentary, for the sake of the simplicity of analysis, it is assumed that the fault current I_{m_b} remains A, as shown in (6). Thus, the reverse recovery duration Δt undertook by the thyristor T_{m2} is as follows:

$$\Delta t = CB/A \tag{12}$$

$$\Delta t > t_r. \tag{13}$$

The duration Δt should be longer than t_r to ensure that the thyristor T_{m2} is turned OFF reliably, as shown in (13). Yet there remains one question that both A in (6) and B in (7) are related to timepoint t_2, which means the Δt in (12) is changeable when inductance L_{out} changes. According to (5), the larger the inductance L_{out} is, the smaller the timepoint t_2. Then, A in (6) gets smaller, which means the main branch current after mode V_b is smaller. Meanwhile, B in (7) gets bigger, which means the residual capacitor energy is bigger. As a result, the duration of the reverse voltage Δt in (12) could be longer. Therefore, the fault at the output of the proposed TCB is the most severe one. Finally, the shortest Δt is provided for the thyristor T_{m2} to recover by setting L_{out} to zero, and the reliability is then ensured no matter where the fault occurs.

B. Requirements for the Current Breaking Process After Reclosing

According to modes VII_f and $VIII_f$ in Fig. 2, after reclosing in the forward current breaking process, both an additional half an LC resonance period and the reverse recovery process for the thyristor T_{p2} are needed before the fault current reaches I_{f0} again. Then, (14) could be obtained, where L_{out} remains representing the outer circuit parameter.

$$t_{add} \le \frac{I_{f0}(L_m + L_{out})}{V_s}. \tag{14}$$

Obviously, the larger the L_{out} is, the easier (14) is to be satisfied. By substituting (1) into (14) and setting L_{out} to zero, another requirement of inductance L_p is obtained by

$$L_p \le \frac{(I_{f0}L_m - V_s t_r)^2}{\pi^2 V_s^2 C}. \tag{15}$$

C. Requirements for Protecting Thyristors

Since the thyristors in the main branch need to carry the sum of main branch current and counter current in some cases, they need to be protected from the perspective of the surge current withstanding capability of the thyristor. After comparing all cases, the most severe condition is the mode III_b, where the thyristor T_{m2} will carry the sum of I_{m_b} and the counter current I_{PB_f}. In addition, since capacitor voltage will be bigger after reclosing, the case after reclosing is considered here.

Supposing that the action timepoint of mode III_b is zero, the sum current I_{sum} is (16), where V_{clamp} is the clamping voltage of MOV and is also the final maximum capacitor voltage before reclosing. V_{clamp} is normally 1.2–2 times of the source voltage.

$$I_{sum} = I_{PB\_f} + I_{m\_b} = \frac{V_{clamp}\sqrt{C}}{\sqrt{L_p}} \sin \frac{t}{\sqrt{L_p C}} + I_{f0} + \frac{V_s}{L_m} t. \tag{16}$$

By deriving (16), (17) is obtained. Since the maximum value of I_{sum} is in the first half-cycle of the sine wave, the range of time t is added in the following:

$$I'_{sum} = \frac{V_{clamp}}{L_p} \cos \frac{t}{\sqrt{L_p C}} + \frac{V_s}{L_m}, t \in (0, \pi\sqrt{L_p C}). \tag{17}$$

Then, the timepoint t_{max} when the derivative of I_{sum} equals to 0 can be obtained according to

$$t_{max} = t|_{I'_{sum}=0}. \tag{18}$$

The maximum value of I_{sum} (I_{sum_max}) should be smaller than the surge current of thyristor (I_{surge}), as shown in the following:

$$I_{sum\_max} < I_{surge}. \tag{19}$$

D. Resistance R_g and Capacitance C

Resistance R_g should be selected for the proposed TCB. The only function of resistor R_g is to charge capacitor C. Yet there remain the following three issues worth considering.

1) According to modes II_f and II_b, the capacitor C will discharge from resistor R_g after a fault.
2) RCB_g needs to break the leakage current caused by R_g.
3) Before the first current breaking process, the capacitor C needs to be charged through the resistor from the source.

Based on the above three issues, resistance R_g should be large enough, but not exceedingly large; otherwise, it will cause the capacitor charging time to be extensive. As a result, R_g is recommended to be selected in the order of 10^4–10^6 Ω according to different dc microgrids. Since the capacitance value is generally tens of μF in the LC resonance method, the maximum charging time is tens of seconds if R_g is in this order, which is reasonable from the view of long normal operating mode. The second issue is also solved because as stated in [6], RCB could interrupt the leakage current up to 10 A.

After determining the resistor R_g, the capacitance C can be selected according to (20), where τ is the capacitor charging

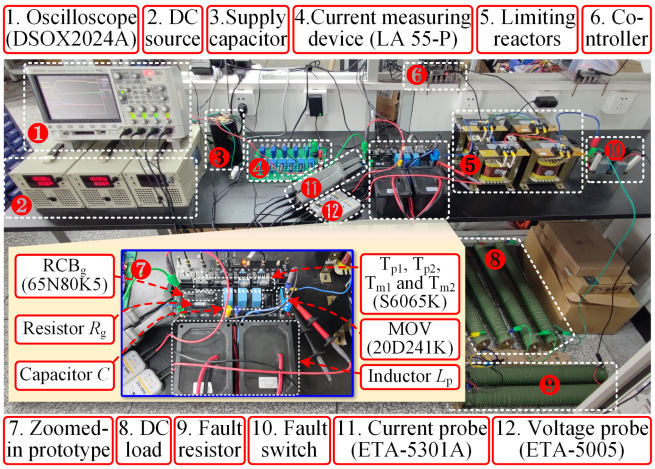

Fig. 6. Scaled-down experimental prototype.

TABLE I
PARAMETERS OF THE PROPOSED TCB

Name	Symbol	Value
Recovery time of thyristor	t_r	70 μs
Preset operation value	I_{f0}	20 A
Resistance	R_g	20 kΩ
Capacitance	C	15 μF
Inductance	L_p	500 μH
Reclosing time	$t_{reclose}$	120 ms

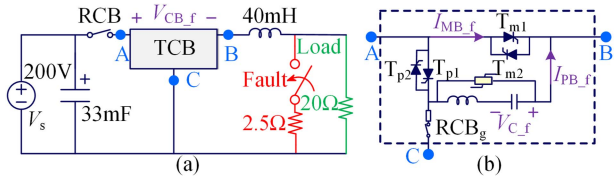

Fig. 7. Experimental circuit for proving forward current breaking functions. (a) DC test system. (b) Connection method.

time constant, ranging from several seconds to several minutes.

$$C = \frac{\tau}{R_g}. \tag{20}$$

E. Design Guidelines

In summary, the proposed TCB could be designed according to the following guidelines.

1) Select thyristors and RCB_g according to the parameters of dc microgrids, such as dc voltage and normal rated current.
2) Determine the preset value I_{f0} and acquire the inductance of inductor L_m, which is placed about SSCB.
3) Determine the resistance R_g according to different dc microgrids, and it is generally in the order of 10^4–$10^6\Omega$.
4) Choose a capacitance C according to (20).
5) Select an inductor L_p based on (13), (15), and (19).

According to the above guidelines, it is obvious that the choosing principles are all dependent on the known parameters rather than the unknown outer circuit parameters. Thus, the reliability of the proposed TCB will not be threatened regardless of the location of the fault. Finally, the security of dc microgrids is ensured.

IV. Experiment Results

To verify the effectiveness of the proposed bidirectional TCB, a scaled-down experimental prototype is established. The overall test platform is shown in Fig. 6, and the zoomed-in prototype picture is in the lower left part of Fig. 6. As shown in Fig. 6, models of the oscilloscope, current measuring device, current probe, and voltage probe are, respectively, DSOX2024A, LA 55-P, ETA-5301A, and ETA-5005. In addition to the measuring devices, the microcontroller TMS320F28335 is selected for sending fault signals and controlling the proposed TCB. As shown in the prototype picture, RCB_g is substituted with the antiseries MOSFETs, the types of which are both 65N80K5. In addition, the model of thyristors is S6065K, and that of MOV is 20D241K. Numerous functions are verified, including the forward and backward current breaking ability, the operating and fault current breaking ability, and the reclosing protection ability. The dc voltage, dc current, and limiting reactor are 200 V, 10 A, and 40 mH, respectively. Parameters of the circuit breaker are presented in Table I. The reclosing time $t_{reclose}$ is 120 ms, which refers to the duration from the timepoint when the fault is successfully detected to the reclosing beginning.

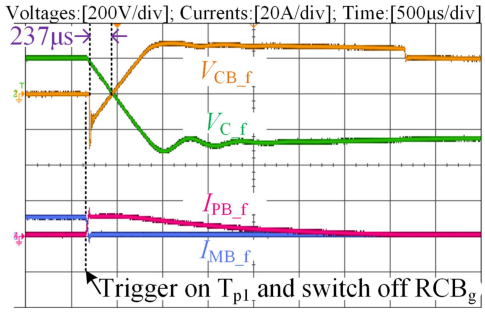

Fig. 8. Waveforms of forward operating current breaking process.

A. Forward Current Breaking Results

The dc test system and its connection method could be found in Fig. 7. Four signals in the forward current condition, including V_{CB_f}, I_{MB_f}, V_{C_f}, and I_{PB_f}, are marked. V_{CB_f} is the circuit breaker voltage and the voltage over the thyristor T_{m1}. I_{MB_f} is the current through thyristor T_{m1}. V_{C_f} is the voltage of capacitor C. I_{PB_f} is the parallel branch current. The operating current breaking results are shown in Fig. 8, and the fault current breaking results are shown in Fig. 9.

1) Operating Current Breaking Results: As shown in Fig. 8, the current I_{MB_f} is 10 A in the normal operating condition. After turning ON the thyristor T_{p1}, the current I_{MB_f} will decrease to 0 A immediately. Then, the reverse recovery process of thyristor T_{p1} lasts 237 μs, which is longer than t_r (70 μs) and ensures turning OFF the thyristor T_{p1} reliably.

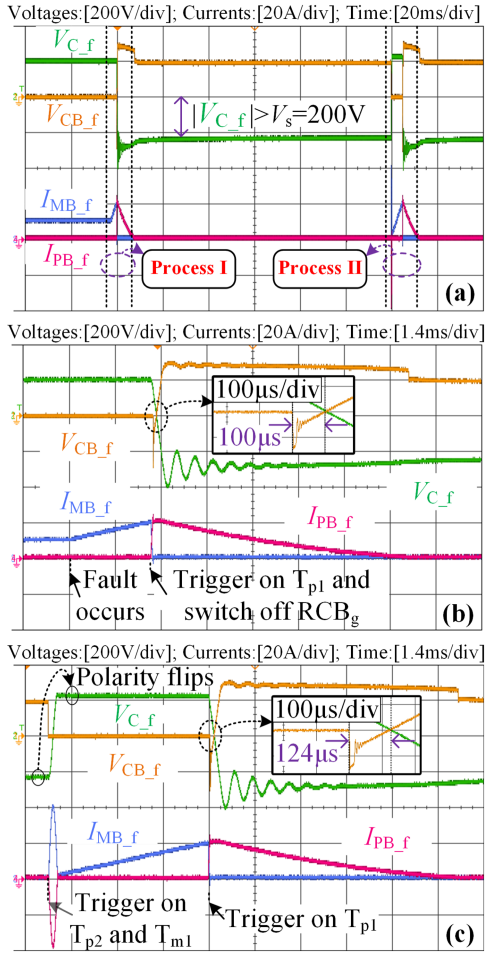

Fig. 9. Waveforms of forward fault current breaking process. (a) Overall experimental results. (b) First current breaking process. (c) Second current breaking process.

2) Fault Current Breaking Results: As shown in Fig. 9, two current breaking processes are done to present the fault current breaking function and the reclosing protection function. After the first current breaking process, the absolute value of capacitor voltage V_{C_f} is bigger than the source voltage V_s, which would ensure sufficient energy to guarantee a reliable current breaking function after reclosing.

In the first current breaking process, the current I_{MB_f} keeps rising after a fault. When I_{MB_f} reaches I_{f0}, the thyristor T_{p1} is turned ON. Then, after current I_{MB_f} decreases to zero, the thyristor T_{m1} undertakes the reverse voltage for 100 μs, and the thyristor T_{m1} is turned OFF successfully.

When the reclosing process starts, turn-ON signals are simultaneously sent to the thyristors T_{m1} and T_{p2}. After half an *LC* resonance period, the polarity of capacitor *C* flips. When I_{MB_f} reaches I_{f0}, the thyristor T_{p1} is turned ON again. Similar to the first current breaking process, current I_{MB_f} decreases to zero, and then the thyristor T_{m1} undertakes the reverse voltage. The difference is that the reverse recovery process of the thyristor T_{m1} lasts 124 μs because the capacitor voltage V_{C_f} in the second breaking process is larger than that in the first one.

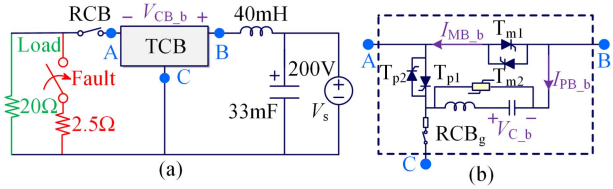

Fig. 10. Experimental circuit for proving backward current breaking functions. (a) DC test system. (b) Connection method.

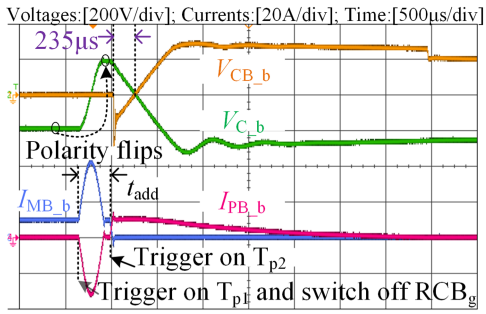

Fig. 11. Waveforms of backward operating current breaking process.

B. Backward Current Breaking Results

The dc test system and its connection method can be found in Fig. 10. Four signals in the backward current condition, including V_{CB_b}, I_{MB_b}, V_{C_b}, and I_{PB_b}, are marked. Their physical meanings are similar to those of the symbols in Fig. 7, but the direction is opposite. The backward operating current breaking results are shown in Fig. 11, and the backward fault current breaking results are shown in Fig. 12.

1) Operating Current Breaking Results: As shown in Fig. 11, the current I_{MB_b} is 10 A in the normal operating condition. When deciding to break the operating current, the thyristor T_{p1} is turned ON. Then, the polarity of capacitor *C* flips after half an *LC* resonance period, and a short recovery duration for the thyristor T_{p1} is needed. The sum of half an *LC* resonance period and this short duration is t_{add}, as marked in Fig. 11. After t_{add}, the thyristor T_{p2} is turned ON. Then the current I_{MB_b} gradually decreases to 0 A. Finally, the thyristor T_{m2} undertakes the reverse voltage for 235 μs and is turned OFF successfully.

2) Fault Current Breaking Results: As shown in Fig. 12, there are also two current breaking processes. The polarity of capacitor *C* has automatically resorted to the initial state after the first current breaking process to prepare for the second one. In addition, the capacitor voltage V_{C_b} is also bigger than the source voltage V_s.

In the first current breaking process, the current I_{MB_b} keeps rising after fault. When I_{MB_b} reaches I_{f0}, the thyristor T_{p1} is turned ON. Similar to the operating current breaking process, a duration t_{add} is needed for flipping the capacitor polarity and turning OFF the thyristor T_{p1}. Then, the thyristor T_{p2} is turned ON. Finally, the thyristor T_{m2} recovers to an insulation state in 80 μs. Compared with the forward current condition, the reverse voltage duration reduces by 20 μs. Fortunately, the proposed

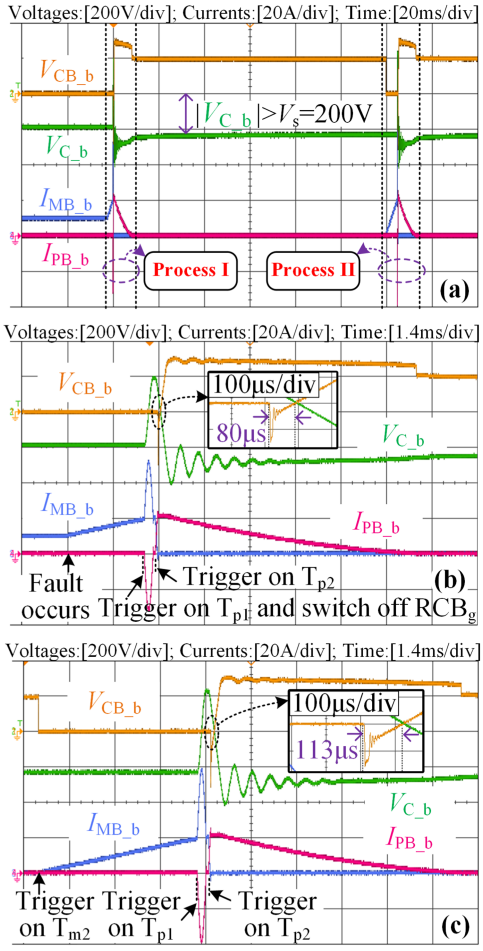

Fig. 12. Waveforms of backward fault current breaking process. (a) Overall experimental results. (b) First current breaking process. (c) Second current breaking process.

TCB also guarantees reliable current breaking function in this condition.

The action sequences of the second current breaking process are like those of the first one, and the thyristor T_{m2} is also successfully turned OFF in 113 μs.

C. Efficiency Testing Results of the Proposed TCB

The efficiency of the proposed TCB is tested here. By setting the dc source voltage to V_s, the output power P_{out} can change as a dc load changes. In this testing experiment, the output power ranges from 1200 to 2000 W. In normal operating condition, the power loss of the thyristor P_{thy} is the conduction loss. The thyristor type is S6065KTP. P_{thy} at different output power level could be calculated after testing its conducting voltage. Then, the system efficiency could be obtained, as shown in Fig. 13. It could be seen that the system efficiency remains over 99.47% when output power ranges from 1200 to 2000 W.

V. Comparison Study

To highlight the advantages of the proposed TCB, the comparison studies are presented in this section.

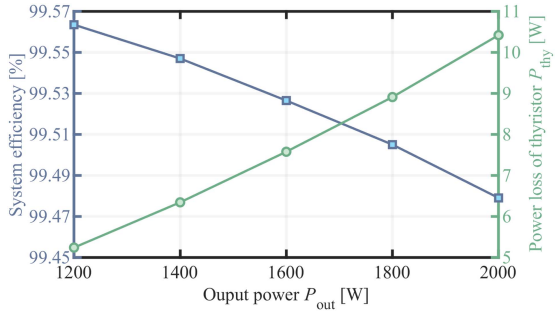

Fig. 13. Curves of power loss of thyristor and system efficiency.

A. Compared With SSCBs Based on Thyristors

Ten TCBs in [15], [16], [19], [20], [21], [22], [23], [24], [25], and [26] are chosen to compare with the proposed TCB shown in Fig. 1, and the results are given in Table II. It is simple to find that the number of components used in the proposed TCB is relatively small, which indicates that the proposed TCB has the advantages including simple circuit design and low construction cost. In addition, compared with the existing TCBs, the proposed TCB exhibits better performance in three aspects.

1) *Conducting Devices (corresponding to conduction loss):* Because there is only one set of parallel thyristors used in the main branch, the conduction loss of the proposed bidirectional TCB is extremely low. Thus, high efficiency is ensured. The conduction losses of inductors are not considered here because they partly take the role of limiting reactors.
2) *Full Controllability and High Reliability:* The proposed TCB uses auxiliary thyristors to actively turn OFF the thyristors in the main branch, and the proposed TCB could interrupt the operating current and fault current with the same procedures. Thus, the proposed TCB has full controllability. In addition, as the proposed TCB can break the fault current in the most severe condition, the proposed TCB always guarantees reliability no matter where the fault is.
3) *Reliable Fast-Reclosing Protection Function:* For improving the practicality, circuit breakers need fast-reclosing protection ability. The proposed TCB always has such an ability after the first current breaking process. The TCBs in [22], [23], and [26] are considered to have an unreliable fast-reclosing protection function. The reason is that the auxiliary thyristors may not be turned OFF reliably before reclosing due to the existence of leakage current flowing through the resistors connecting to the ground. In addition, the capacitor in the TCB in [21] needs long time to discharge after the first current breaking process because it discharges through an enormous resistor. Thus, it has the reclosing protection function but not a fast one.

B. Compared With SSCBs Based on Full-Controllable Devices

To present a more comprehensive comparison, the proposed TCB is compared with the SSCBs based on IGBT, GTO, and

TABLE II
COMPARISON OF DIFFERENT BIDIRECTIONAL THYRISTOR-BASED SSCBS

	[15]	[16]	[19]	[20]	[21]	[22]	[23]	[24]	[25]	[26]	**Proposed**
Number of thyristors	2	2	3	5	4	3	3	6	4	6	**4**
Number of diodes	2	3	2	2	5	3	3	0	0	2	**0**
Number of capacitors	5	1	2	1	2	1	1	1	2	1	**1**
Number of inductors (1)	2	1	2	1	0	1	1	0	0	1	**1**
Number of resistors	2	2	2	0	3	2	2	2	2	2	**1**
Number of MOV	0	2	1	0	2	1	1	1	1	0	**1**
Number of mechanical switches	1	0	1	0	0	0	0	1	0	0	**1**
Conducting devices (2)	1T+1D	1T+1D	1T+1D	1T+1D	1T	1T+1D	1T+1D	2T	1T	1T	**1T**
Full controllability	No	No	Yes	Yes	Yes	Yes	Yes	Yes	Yes	Yes	**Yes**
High reliability	No	No	No	No	No	Yes	Yes	Yes	Yes	Yes	**Yes**
Reliable fast-reclosing protection function	No	No	No	No	No	No	No	Yes	No	No	**Yes**

(1) Inductors include discrete inductors and coupled inductors. (2) T represents thyristor and D represents diode.

TABLE III
FEATURES OF DIFFERENT POWER ELECTRONICS DEVICES USED IN SSCBS

	Diode	Thyristor	IGBT	GTO	IGCT
Model	VS-SD11 00C30C	C783CP	FZ1500R 33HE3	5SGA40L 4501	5SHY35L 4520
Structure	Three in parallel	Two in parallel (2)	Two in parallel	Three in parallel	Two in parallel
On-state voltage (1)	1.32 V	1.60 V	2.55 V(I) 3.10 V(D)	2.47 V	1.65 V
Cost	$290.37 (1.0 p.u.)	$1245.78 (4.3 p.u.)	$4690.14 (16.1 p.u.)	$7631.70 (26.3 p.u.)	$6384.70 (22.0 p.u.)

(1) IGBT here has an internal diode. I represents IGBT, and D represents diode.

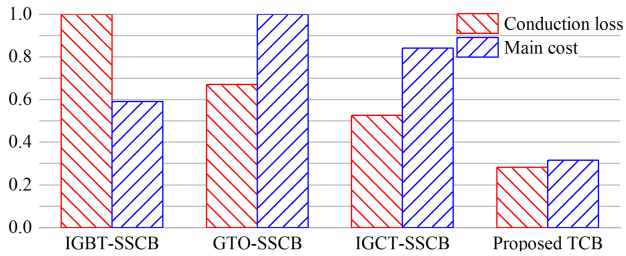

Fig. 14. Relative conduction loss and main cost of four SSCBs.

IGCT in the 1.5 kV/4.5 MW system. Such a voltage level is the same as that of some city subway systems [9], and nearly two times voltage margin is needed for equipment safety. The features of these fully controlled devices used in the SSCBs are given in Table III. According to the data given in Table III, the conduction loss and the power electronics devices' cost of the different SSCBs can be calculated.

1) *Conduction Loss Calculation:* For the SSCBs based on full-controllable devices, the operating current normally flows through the one diode and one main switch (i.e., IGBT, GTO, or IGCT) [9]. Different from these SSCBs, the operating current only flows through one thyristor in the main branch. According to Table III, the conduction loss is 4.80 kW for the proposed TCB. The overall efficiency of one single proposed topology is 99.89%. In addition, the conduction loss and efficiency of the other three SSCBs could also be calculated. The conduction losses are 16.95 (IGBT-SSCB), 11.37 (GTO-SSCB), and 8.91 kW (IGCT-SSCB), and the efficiencies are 99.62% (IGBT-SSCB), 99.75% (GTO-SSCB), and 99.80% (IGCT-SSCB). Compared with the other three SSCBs, the proposed TCB is the most effective one. With the establishment of large-scale dc microgrids, the need of breakers is paramount because breakers are generally needed to be installed in two sides of every dc line. The power losses of the whole dc microgrids could be limited to a low level with the use of the proposed TCB.
2) *Power Electronics Devices Cost (main cost):* For the *LC* resonance method, small capacitance capacitors can excite large currents through small inductance reactors. Thus, the commutating branch using the *LC* resonance method will normally not increase the construction cost noticeably, which is one reason why the *LC* resonance method is widely used. Therefore, power electronics cost is the main cost of SSCBs, and they are calculated here according to Table III. They are 32.2 per unit (p.u.) (IGBT-SSCB), 54.6 p.u. (GTO-SSCB), 46.0 p.u. (IGCT-SSCB), and 17.2 p.u. (proposed TCB).

Furthermore, the relative conduction loss and main cost are shown in Fig. 14. It is easily found that the proposed method has the lowest conduction loss and main cost in four SSCBs, which demonstrates the proposed TCB as effective and economical. Thus, the proposed TCB is much more suitable to protect the dc microgrids.

VI. CONCLUSION

A novel thyristor-based SSCB was proposed in this article to protect dc microgrids. It was a bidirectional topology with low conduction loss. By masterly using an *LC* resonant circuit and proper control orders, the proposed TCB could break both operating and fault currents actively and reliably. As shown in the experiments, even in the most severe backward fault current breaking case, the proposed TCB could ensure enough duration ($80\ \mu s > t_r$) for turning OFF the thyristor T_{m2}. Hence, the proposed TCB had full controllability and high reliability. In addition, in both the forward and backward current breaking experiment results, the absolute value of capacitor voltage was higher than the source voltage V_s after the first current breaking process. Then, through appropriate control orders, the reclosing protection ability was also ensured. As a result, the proposed

TCB was one superior candidate for protecting dc microgrids. Using an *LC* resonant circuit to realize the fast-reclosing protection function was one major contribution of the proposed TCB. Detailed operation principles and parameters guidelines were presented. Finally, the superior performance of the proposed TCB was further illustrated by the comparison analyses. Compared with the three SSCBs based on full-controllable devices (i.e., IGBT, IGCT, and GTO), the proposed TCB could guarantee the advantages of both lower conduction loss and construction cost. The conduction loss of the proposed TCB was only 28.3% of that of the IGBT-SSCB, and the main cost was about 53.4%.

References

[1] Y. Shan, J. Hu, M. Liu, J. Zhu, and J. M. Guerrero, "Model predictive voltage and power control of islanded PV-battery microgrids with washout-filter-based power sharing strategy," *IEEE Trans. Power Electron.*, vol. 35, no. 2, pp. 1227–1238, Feb. 2020.

[2] S. Beheshtaein, R. M. Cuzner, M. Forouzesh, M. Savaghebi, and J. M. Guerrero, "DC microgrid protection: A comprehensive review," *IEEE Trans. Emerg. Sel. Topics Power Electron.*, early access, doi: 10.1109/JESTPE.2019.2904588.

[3] K. Qin, S. Wang, J. Ma, J. Shu, R. Zhang, and T. Liu, "Thyristor-based DCCB with reliable fast reclosing protection ability by restoring capacitor polarity," *IEEE Trans. Power Electron.*, vol. 38, no. 6, pp. 7760–7770, Jun. 2023, doi: 10.1109/TPEL.2023.3250093.

[4] N. Hou, Y. Zhang, and Y. W. Li, "A load-current-estimating scheme with delay compensation for the dual-active-bridge DC–DC converter," *IEEE Trans. Power Electron.*, vol. 37, no. 3, pp. 2636–2647, Mar. 2022.

[5] N. Hou and Y. W. Li, "Overview and comparison of modulation and control strategies for a nonresonant single-phase dual-active-bridge DC–DC converter," *IEEE Trans. Power Electron.*, vol. 35, no. 3, pp. 3148–3172, Mar. 2020.

[6] K. Qin, S. Wang, J. Ma, J. Shu, J. Zhou, and T. Liu, "A new thyristor-based DC circuit breaker using diode clamping switching," *IEEE Trans. Power Electron.*, vol. 37, no. 8, pp. 8773–8779, Aug. 2022.

[7] J. Shu, S. Wang, J. Ma, T. Liu, and Z. He, "An active Z-source DC circuit breaker combined with SCR and IGBT," *IEEE Trans. Power Electron.*, vol. 35, no. 10, pp. 10003–10007, Oct. 2020.

[8] X. Xu, W. Chen, C. Liu, R. Sun, Z. Li, and B. Zhang, "An efficient and reliable solid-state circuit breaker based on mixture device," *IEEE Trans. Power Electron.*, vol. 36, no. 9, pp. 9767–9771, Sep. 2021.

[9] X. Xu, J. Ye, Y. Wang, X. Xu, Z. Lai, and X. Wei, "Design of a reliable bidirectional solid-state circuit breaker for DC microgrids," *IEEE Trans. Power Electron.*, vol. 37, no. 6, pp. 7200–7208, Jun. 2022.

[10] Y. Ren, X. Yang, F. Zhang, F. Wang, L. M. Tolbert, and Y. Pei, "A single gate driver based solid-state circuit breaker using series connected SiC MOSFETs," *IEEE Trans. Power Electron.*, vol. 34, no. 3, pp. 2002–2006, Mar. 2019.

[11] X. Song, P. Cairoli, Y. Du, and A. Antoniazzi, "A review of thyristor based DC solid-state circuit breakers," *IEEE Open J. Power Electron.*, vol. 2, pp. 659–672, 2021.

[12] K. A. Corzine and R. W. Ashton, "A new Z-source DC circuit breaker," *IEEE Trans. Power Electron.*, vol. 27, no. 6, pp. 2796–2804, Jun. 2012.

[13] W. Li, Y. Wang, X. Wu, and X. Zhang, "A novel solid-state circuit breaker for on-board DC microgrid system," *IEEE Trans. Ind. Electron.*, vol. 66, no. 7, pp. 5715–5723, Jul. 2019.

[14] V. R. I, S. N. Banavath, and S. Thamballa, "Modified Z-source DC circuit breaker with enhanced performance during commissioning and reclosing," *IEEE Trans. Power Electron.*, vol. 37, no. 1, pp. 910–919, Jan. 2022.

[15] D. Keshavarzi, T. Ghanbari, and E. Farjah, "A Z-source-based bidirectional DC circuit breaker with fault current limitation and interruption capabilities," *IEEE Trans. Power Electron.*, vol. 32, no. 9, pp. 6813–6822, Sep. 2017.

[16] Z. Zhou, J. Jiang, S. Ye, C. Liu, and D. Zhang, "A Γ-source circuit breaker for DC microgrid protection," *IEEE Trans. Ind. Electron.*, vol. 68, no. 3, pp. 2310–2320, Mar. 2021.

[17] S. G. Savaliya and B. G. Fernandes, "Modified bi-directional Z-source breaker with reclosing and rebreaking capabilities," in *Proc. IEEE Appl. Power Electron. Conf. Expo.*, 2018, pp. 3497–3504.

[18] Y. Yang and C. Huang, "A low-loss Z-source circuit breaker for LVDC systems," *IEEE Trans. Emerg. Sel. Topics Power Electron.*, vol. 9, no. 3, pp. 2518–2528, Jun. 2021.

[19] Z. Zhou, M. Chen, J. Jiang, D. Zhang, S. Ye, and C. Liu, "Analysis and design of a novel thyristor-based circuit breaker for DC microgrids," *IEEE Trans. Power Electron.*, vol. 35, no. 3, pp. 2959–2968, Mar. 2020.

[20] I. V. Raghavendra, S. N. Banavath, C. N. M. Ajmal, and A. Ray, "Modular bidirectional solid-state DC circuit breaker for next-generation electric aircrafts," *IEEE J. Emerg. Sel. Topics Power Electron.*, vol. 10, no. 5, pp. 5486–5497, Oct. 2022.

[21] R. Kheirollahi et al., "Fast Y-type thyristor-based DC SSCB using complementary commutation in a capacitor–capacitor pair structure," *IEEE Trans. Power Electron.*, vol. 38, no. 1, pp. 1144–1154, Jan. 2023.

[22] X. Xu, J. Ye, Y. Wang, X. Xu, Z. Lai, and X. Wei, "Design of a reliable bidirectional solid-state circuit breaker for DC microgrids," *IEEE Trans. Power Electron.*, vol. 37, no. 6, pp. 7200–7208, Jun. 2022.

[23] X. Xu et al., "A novel thyristor-based bidirectional SSCB with controllable current breaking capability," *IEEE Trans. Power Electron.*, vol. 37, no. 4, pp. 4526–4534, Apr. 2022.

[24] M. Marwaha et al., "SCR-based bidirectional circuit breaker for DC system protection with soft reclosing capability," *IEEE Trans. Ind. Electron.*, vol. 70, no. 5, pp. 4739–4750, May 2023.

[25] J. Shu, J. Ma, S. Wang, Y. Dong, T. Liu, and Z. He, "A new active thyristor-based DCCB with reliable opening process," *IEEE Trans. Power Electron.*, vol. 36, no. 4, pp. 3617–3621, Apr. 2021.

[26] Z. Ayubu, J.-Y. Kim, J.-Y. Yu, S.-M. Song, and I.-D. Kim, "Novel bidirectional DC solid-state circuit breaker with operating duty capability," *IEEE Trans. Ind. Electron.*, vol. 68, no. 10, pp. 9104–9113, Oct. 2021.

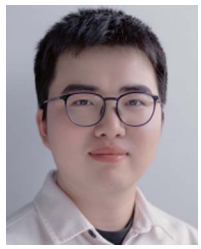

Kejun Qin (Student Member, IEEE) received the B.S. degree in electrical engineering from Southwest Jiaotong University, Chengdu, China, in 2020, and the M.S. degree in electrical engineering from Sichuan University, Chengdu, in 2023.

His research interests include power electronics and dc circuit breaker.

Shunliang Wang (Member, IEEE) received the B.S. and Ph.D. degrees in electrical engineering from Southwest Jiaotong University, Chengdu, China, in 2010 and 2016, respectively.

From 2017 to 2018, he was a Visiting Scholar with the Department of Energy Technology, Aalborg University, Aalborg, Denmark. He is currently an Associate Professor with the College of Electrical Engineering, Sichuan University, Chengdu, China. His current research interests include high-voltage direct current transmission (HVdc), power electronics-based power system, topology, control, modulation, and modeling of power converters.

Dr. Wang was the recipient of the Best Paper Award at the IEEE International Electrical and Energy Conference (CIEEC) 2019 and the 18th international conference on ac and dc Power Transmission (ACDC) 2022, and the Outstanding Young Person Award for dc Power from the Chinese Society of Electrical Engineering.

Junpeng Ma (Member, IEEE) received the B.S. and Ph.D. degrees in electrical engineering from Southwest Jiaotong University, Chengdu, China, in 2013 and 2018, respectively.

From 2017 to 2018, he was a Guest Ph.D. Student with Aalborg University, Aalborg, Denmark. He is currently an Associate Professor with Sichuan University, Chengdu. His research interests include the modeling and control of grid-connected converters applied in the new energy, and the HVdc systems.

Dr. Ma was the recipient of the Best Paper Award from the International Conference twice.

Ji Shu received the B.S. and M.S. degrees in electrical engineering from Sichuan University, Chengdu, China, in 2018 and 2021, respectively. He is currently working toward the Ph.D. degree in electronic and computer engineering with The Hong Kong University of Science and Technology, Hong Kong, China.

His research interests include dc system protection, next-generation power conversion, and the wide-bandgap power semiconductor devices.

Rui Zhang (Student Member, IEEE) received the B.S. and M.S. degrees in electrical engineering in 2015 and 2018, respectively. from Sichuan University, Chengdu, China, where he is currently working toward the Ph.D. degree in electrical engineering with the College of Electrical Engineering.

His research interests include power electronics, renewable energy power generation system, and electromagnetic transient simulation.

Tianqi Liu (Senior Member, IEEE) received the B.S. and M.S. degrees from Sichuan University, Chengdu, China, in 1982 and 1986, respectively, and the Ph.D. degree from Chongqing University, Chongqing, China, in 1996, all in electrical engineering.

She is currently a Professor with the College of Electrical Engineering, Sichuan University. Her research interests include power system analysis and stability control, HVdc, optimal operation, dynamic security analysis, dynamic state estimation, and the load forecast.